Thermodynamics of heavy quarkonium in rotating matter from holography

Jing Zhou[1,*], Xun Chen[2,†], Yan-Qing Zhao[2,‡] and Jialun Ping[1,§]

[1]*Department of Physics, Nanjing Normal University, Nanjing, Jiangsu 210097, China*
[2]*Key Laboratory of Quark and Lepton Physics (MOE) and Institute of Particle Physics,
Central China Normal University, Wuhan 430079, China*

Using the guage/gravity correspondence, we study the free energy, entropy, binding energy, and internal energy of a heavy quarkonium in the rotating quark-gluon plasma (QGP). First, we extend the static black hole with planar horizon to the spinning case, which is dual to the rotating matter. Subsequently, we use the Wilson loop to get the free energy of heavy quarkonium. Entropy, binding energy, and internal energy are naturally given by the thermodynamic relationship. It is found that angular velocity will suppress the dissociation temperature of heavy quarkonium and change the system from confined to deconfined phase with the increase of angular velocity. Thus, the heavy quarkonium will dissolve at a certain separating distance in the deconfined phase. We also compare these thermodynamic quantities of the quark-antiquark pair in the direction parallel and transverse to the rotation direction. At last, the free energy, entropy, and internal energy of a single quark are discussed. It is found that these quantities are decreasing functions of temperature.

I. INTRODUCTION

It is well known that a new state of matter, the so-called quark gluon plasma (QGP), was formed at the Relativistic Heavy Ion Collider (RHIC) and the Large Hadron Collider (LHC) [1–4]. Heavy quarkonium, which is a bound state of a quark and antiquark, is among the most sensitive probes used in the experimental to study the properties of QGP. Depending on the size of the quarkonium state and on the temperature of the plasma, the heavy quark and antiquark may be screened from each other, affecting the production rates of heavy quarkonia in heavy-ion collisions [5–7]. The static potential of two infinitely heavy quarks and their free energy play an important role in the theoretical description of color screening. The bound state of the heavy quarks is assumed to strongly entangle with the rest of the statistical system, which will lead to large amount of entropy with the increase of the interquark distance L; see Refs. [8–10] for lattice results. In recent years, the induced entropic force $F_e = T\partial S/\partial L$ (T is temperature) is considered to have contribution on the quarkonium suppression [11–20].

From relativistic heavy-ion collision experiments, we know the QCD matter created in typical noncentral collision events will carry a nonzero angular momentum

on the order of 10^4–$10^5\hbar$ with local angular velocity in the range of 0.01–0.1 GeV [21–27]. Large values of the initial angular momentum of the plasma may give rise to significant observable effects. For instance, a finite angular momentum will enhance the elliptic flow coefficient, broaden the transverse momentum spectra and lead to the polarization of the emitted hadrons and fluid vorticity.

The AdS/CFT correspondence, proposed by Maldacena, has become a valuable method for studying strongly coupled gauge theories [28–30]. One of the most promising applications of the gauge/gravity correspondence (or more generally AdS/CFT) concerns the physics of hot, strongly coupled gauge theory plasmas; see Refs. [31,32] for a review. The plasmas described in this way are expected to have many properties in common with the realistic QGP created in the relativistic heavy-ion collisions, and the latter indeed has been found to be strongly coupled at the experimentally accessible temperatures somewhat above the critical temperature [1–4]. However, a conformal theory cannot fully describe a real QCD theory. The holographic approach can be made more realistic in two ways. One is based on adopting a more sophisticated gravity model in the bulk, such as a deformed anti–de Sitter–Reissner–Nordström (AdS/RN) model [33–37] and Einstein-Maxwell-Dilaton model [38–43]. The other way is to use more complex black-hole spacetimes to model aspects of the QGP.

One of the important aspects is the angular momentum of the QGP. As discussed in Ref. [44], the angular momentum of an asymptotically AdS black hole does have

---
[*]171001005@njnu.edu.cn
[†]Corresponding author.
chenxunhep@qq.com
[‡]yanqzhao@qq.com
[§]Corresponding author.
jlping@njnu.edu.cn

a holographic interpretation, arising from the frame-dragging effect [45]. Frame dragging at infinity, described by a rotational parameter giving the angular momentum per unit mass of the bulk black hole, reproduces the motion of the fluid on the boundary as a simple rotation [46,47] or more complex shearing [48–51]. Following Refs. [52–57], we want to extend the black hole with a planar horizon to the spinning case in this paper instead of using a Kerr-AdS black hole with a spherical horizon. The main reason is the near-horizon limit of the D3-brane gives the black hole with planar horizon from AdS/CFT. More discussions can be found in Ref. [58].

The rest of this paper is organized as follow. In Sec. II, we extend the deformed AdS Schwarzschild black hole to rotating black holes with planar horizon. In Sec. III, we calculate the results of quark-antiquark distante, free energy, entropy, binding energy, and internal energy numerically in a rotating deformed AdS Schwarzschild black hole. The free energy, entropy, and internal energy of a single quark have been calculated in Sec. IV. Finally, the conclusion and discussion will be given in Sec. V.

II. SETUP

The solution of the five-dimensional gravity action with a negative cosmological constant is known as the AdS Schwarzschild black hole. Since a conformal theory cannot describe the meson spectrum well, a deformed AdS Schwarzschild black-hole metric is introduced in some papers [33,36,38],

$$ds^2 = \frac{L_{Ads}^2 h(z)}{z^2}\left(-f(z)dt^2 + d\vec{x}^2 + \frac{dz^2}{f(z)}\right), \quad (1)$$

$$f(z) = 1 - \frac{z^4}{z_h^4}, \quad (2)$$

where $h(z) = \exp(cz^2/2)$ is called the warp factor, which determines the characteristics of the soft wall model, and c determines the deviation from conformality. We take $c \approx 0.9$ GeV^2 and L_{AdS} to be 1 [35]. z_h is the position of black-hole horizon, $\vec{x}$ is the three-dimensional directions of the space, and z is the fifth holographic coordinate. Following Refs. [54–57], we extend the deformed AdS Schwarzschild black hole to the rotating case. Through transforming the Poincaré coordinate to the cylindrical coordinate and the standard Lorentz transformation in the ϕ direction, we have

$$t \rightarrow \frac{1}{\sqrt{1 - \omega^2 l^2}}(t + \omega l^2 \phi), \quad (3)$$

$$\phi \rightarrow \frac{1}{\sqrt{1 - \omega^2 l^2}}(\phi + \omega t). \quad (4)$$

Here, ω is the angular velocity, and l is the radius of the rotating axis. In Ref. [59], the author estimated that the size of QGP at the RHIC and LHC will be around 4–8 and 6–11 fm, respectively. Thus, we fix the rotating radius as $l = 10$ GeV$^{-1} \sim 2$ fm. Then, we extend the deformed AdS/RN black hole to a rotating one with a planar horizon. The general metric is as follows,

$$ds^2 = g_{tt}dt^2 + g_{t\phi}dtd\phi + g_{\phi t}d\phi dt + g_{\phi\phi}l^2 d\phi^2$$
$$+ g_{zz}dz^2 + g_{xx}\sum_{i=1}^{2} dx_i^2 \quad (5)$$

for our metric,

$$g_{tt} = H(z)\gamma^2(\omega^2 l^2 - f(z)), \quad (6)$$

$$g_{\phi\phi} = H(z)\gamma^2(1 - \omega^2 f(z)l^2), \quad (7)$$

$$g_{t\phi} = g_{\phi t} = H(z)\gamma^2\omega(1 - f(z))l^2, \quad (8)$$

$$g_{zz} = \frac{H(z)}{f(z)}, \quad (9)$$

$$g_{xx} = H(z), \quad (10)$$

$$\gamma = \frac{1}{\sqrt{1 - \omega^2 l^2}}. \quad (11)$$

Then, we can rewrite the rotating metric as follows,

$$ds^2 = -N(z)dt^2 + \frac{H(z)dz^2}{F(z)} + R(z)(d\phi + P(z)dt)^2$$
$$+ H(z)\sum_{i=1}^{2} dx_i^2, \quad (12)$$

where

$$N(z) = \frac{H(z)f(z)(1 - \omega^2 l^2)}{1 - f(z)\omega^2 l^2}, \quad (13)$$

$$R(z) = H(z)\gamma^2 l^2 - H(z)f(z)\gamma^2\omega^2 l^4, \quad (14)$$

$$P(z) = \frac{\omega - f(z)\omega}{1 - f(z)\omega^2 l^2}, \quad (15)$$

and we have set

$$H(z) = \frac{h(z)}{z^2},$$

$$\gamma = \frac{1}{\sqrt{1 - \omega^2 l^2}}.$$

We define $\hat{g}_{00} = -N(z)$ and the $z - z$ component of the inverse of metric as g^{11}. The Hawking temperature of the rotating black hole can be given as

$$T = \left| \frac{\kappa}{2\pi} \right| = \left| \frac{\lim_{z \to z_h} -\frac{1}{2}\sqrt{\frac{g^{11}}{-\hat{g}_{00}}}\hat{g}_{00,1}}{2\pi} \right| = \frac{1}{\pi z_h}\sqrt{1 - \omega^2}, \quad (16)$$

where κ is the surface gravity. Then, we put a static heavy quark-antiquark pair in that rotating background. For the rotating quark or quark-antiquark pair, we may refer to Refs. [60–62]. The Nambu-Goto action of the worldsheet in the metric

$$S_{\mathrm{NG}} = -\frac{1}{2\pi\alpha'}\int d^2\xi\sqrt{-\det g_{ab}}, \quad (17)$$

where $\frac{1}{2\pi\alpha'}$ is the string tension and g_{ab} is the induced metric,

$$g_{ab} = g_{MN}\partial_a X^M \partial_b X^N, \quad a, b = 0, 1. \quad (18)$$

We define X^M and g_{MN} are the coordinates and the metric of the AdS space. Then, we can parametrize worldsheet coordinates with $\xi^0 = t$, $\xi^1 = x_1$, which means the string is transverse to rotation direction. So, the Nambu-Goto action can be rewritten as

$$S_{\mathrm{NG}} = -\frac{1}{2\pi\alpha' T}\int_{-L/2}^{L/2} d\xi^1 \sqrt{k_1(z)\frac{dz^2}{d\xi^{12}} + k_2(z)}. \quad (19)$$

For transverse direction, $k_1(z)$ and $k_2(z)$ are

$$k_1(z) = k_1^{tra}(z) = \frac{(N(z) - R(z)P(z)^2)H(z)}{f(z)}, \quad (20)$$

$$k_2(z) = k_2^{tra}(z) = -(R(z)P(z)^2 - N(z))H(z). \quad (21)$$

For parallel direction, we can parametrize worldsheet coordinates with $\xi^0 = t$, $\xi^1 = l\phi$. Then, $k_1(z)$ and $k_2(z)$ are

$$k_1(z) = k_1^{\mathrm{par}}(z) = \frac{(N(z) - R(z)P(z)^2)H(z)}{f(z)}, \quad (22)$$

$$k_2(z) = k_2^{\mathrm{par}}(z) = N(z)R(z). \quad (23)$$

The interquark distance L of the heavy $Q\bar{Q}$ pair can be calculated as

$$L = 2\int_0^{z_0}\left[\frac{k_2(z)}{k_1(z)}\left(\frac{k_2(z)}{k_2(z_0)} - 1\right)\right]^{-1/2} dz. \quad (24)$$

And the free energy of $Q\bar{Q}$ pair is given as

$$\frac{\pi F_{Q\bar{Q}}}{\sqrt{\lambda}} = \int_0^{z_0} dz\left(\sqrt{\frac{k_2(z)k_1(z)}{k_2(z) - k_2(z_0)}} - \sqrt{k_2(z \to 0)}\right)$$
$$- \int_{z_0}^{\infty}\sqrt{k_2(z \to 0)}dz. \quad (25)$$

Here, we use the minimum subtraction to eliminate the divergence of free energy. The subtracted term is interpreted as the infinite quark and antiquark mass in four-dimensional QCD [36]. This kind of procedure involves a subtracting constant term in the paper. Since the constant is naturally introduced by this procedure, our paper and other papers still keep it. $\sqrt{\lambda}$ is defined as $L_{\mathrm{AdS}}^2/\alpha'$; we just set it to 1, since we mainly focus on the qualitative behavior in this paper. The counterterm can be calculated as $\frac{1}{z^2}$. The entropy of $Q\bar{Q}$ pair is defined as

$$S_{Q\bar{Q}} = -\partial F_{Q\bar{Q}}/\partial T, \quad (26)$$

where T is the temperature of the QGP. For a single quark, the integral range is from 0 to z_h. Then, we have

$$F_Q = \frac{1}{2\pi}\left(\int_0^{z_h} dz\left(\sqrt{k_1(z)} - \frac{1}{z^2}\right) - \frac{1}{z_h}\right). \quad (27)$$

The horizon position is often calculated by setting $f(z_h) = 0$, However, we note that there is a shift of horizon due to finite angular velocity. According to the Ref. [63], the binding energy is defined as $E_{Q\bar{Q}}(L) = F_{Q\bar{Q}} - 2F_Q$. Thus, the internal energy can be naturally calculated by $U_{Q\bar{Q}}(L, T) = F_{Q\bar{Q}}(L, T) + TS_{Q\bar{Q}}(L, T)$.

III. THERMODYNAMIC QUANTITIES OF HEAVY QUARKONIUM WITH FINITE ANGULAR VELOCITY

The entropy, free energy, binding energy, and internal energy of heavy quark-antiquark pair with finite temperature have been discussed in Ref. [20] by using the Schrödinger equation. Meanwhile, Ref. [63] discussed these thermodynamic quantities in conformal and different noncomformal models from holography. Lattice results with zero and finite temperature can be found in Refs. [64,65]. In Ref. [66], we study these thermodynamic quantities of heavy quark-antiquark pair in the magnetic background. In this paper, we focus on these thermodynamic quantities of heavy quark-antiquark pair, which is put in the rotating matter.

Before that, we first study the dependence of interquark distance L of $Q\bar{Q}$ pair versus z_0 at different $\omega = 0$, 0.01, 0.08 GeV as shown in Fig. 1(a). It is found that the interquark distance L increases with the ω at $\omega = 0$, 0.05 GeV. But for $\omega = 0.08$ GeV, when z_0 increases, the interquark distance L of $Q\bar{Q}$ pair reaches the maximum, then goes down to the zero. It indicates that the $Q\bar{Q}$ pair is
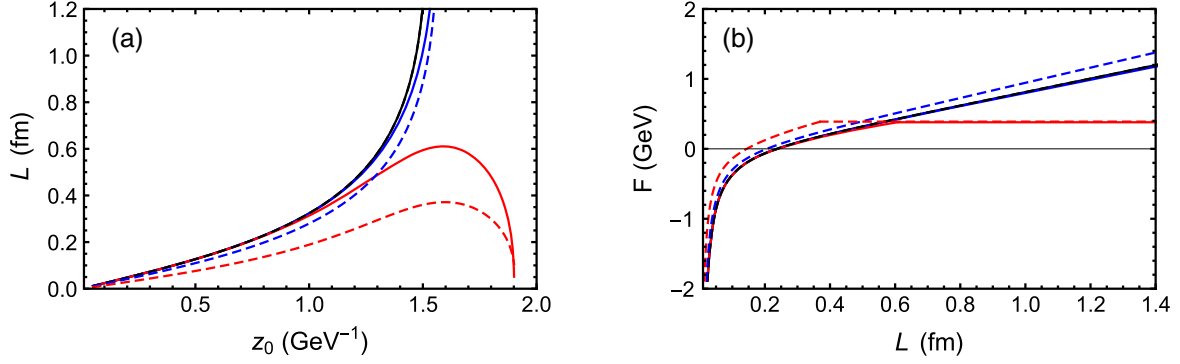
FIG. 1. (a) The dependence of interquark distance L on z_0 at $T = 0.1$ GeV with vanishing chemical potential. The black line is $\omega = 0$, the blue line is $\omega = 0.05$ GeV, and the red line is $\omega = 0.08$ GeV for transverse direction. The black dashed line is $\omega = 0$, the blue dashed line is $\omega = 0.05$ GeV, and the red dashed line is $\omega = 0.08$ GeV for the parallel direction. (b) The dependence of free energy F on interquark distance L at $T = 0.1$ GeV with vanishing chemical potential. The black line is $\omega = 0$, the blue line is $\omega = 0.05$ GeV, and the red line is $\omega = 0.08$ GeV for the transverse direction. The black dashed line is $\omega = 0$, the blue dashed line is $\omega = 0.05$ GeV, and the red dashed line is $\omega = 0.08$ GeV for the parallel direction.

in the confinement phase at small $\omega = 0, 0.05$ GeV and in the deconfinement phase at large $\omega = 0.08$ GeV. In the confinement phase, the U-shape string which connects with quark and antiquark pair always exists. The distance L increases with z_0. In the deconfinement phase, there is a maximum of the interquark distance L, which is the screening distance. Continuing to increase the z_0, U-shape strings become unstable when approaching to horizon; then, it goes down to zero. In parallel direction, the quark-antiquark pair will be screened at smaller distance than that in the transverse direction for $\omega = 0.08$ GeV.

Then, we can numerically calculate the free energy which is given by Eq. (25). In Fig. 1(b), we plot the free energy of the heavy $Q\bar{Q}$ pair as a function of the interquark distance L for different ω. One can find that the free energy grows with L. In the confinement phase, free energy will go to infinity, which means we cannot find a single quark.

For large angular velocity $\omega = 0.08$ GeV, the free energy will reach a maximum at a certain distance then we assume the free energy will become flat. It indicates that the heavy $Q\bar{Q}$ will dissociate at finite distance. Although the quark-antiquark pair will be screened at smaller distance in the parallel direction, the maximum free energy is almost the same for both the transverse and parallel directions at $\omega = 0.08$ GeV.

Using the Eq. (26), we show the dependence of entropy of heavy $Q\bar{Q}$ pair on the interquark distance L of $Q\bar{Q}$ pair at different angular velocities ω in Fig. 2(a). We fix the chemical potential as $\mu = 0$ and the temperature as $T = 0.1$ GeV. Then, one can find that the entropy increases with the increase of the angular velocity ω. We find the maximum entropy is same for both the transverse and parallel directions at $\omega = 0.08$ GeV. As we know, the quick increase will lead to large entropic force, which is also considered as a reason of
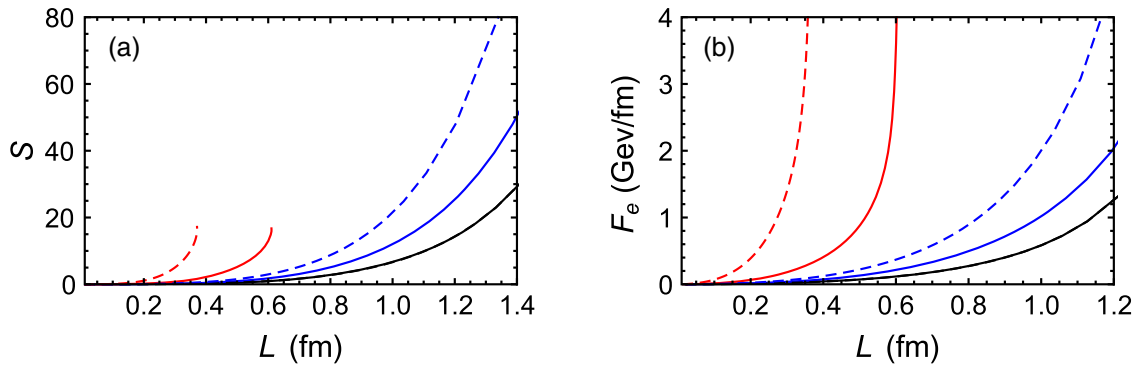

FIG. 2. (a) The dependence of entropy on L for different ω. The chemical potential is 0, and the temperature as $T = 0.1$ GeV. The black line is $\omega = 0$, the blue line is $\omega = 0.05$ GeV, and The red line is $\omega = 0.08$ GeV for the transverse direction. The black dashed line is $\omega = 0$, the blue dashed line is $\omega = 0.05$ GeV, and the red dashed line is $\omega = 0.08$ GeV for the parallel direction. (b) Corresponding entropic force as a function of L. The chemical potential is 0, and the temperature is $T = 0.1$ GeV. The black line is $\omega = 0$, the blue line is $\omega = 0.05$ GeV, and the red line is $\omega = 0.08$ GeV for the transverse direction. The black dashed line is $\omega = 0$, the blue dashed line is $\omega = 0.05$ GeV, and the red dashed line is $\omega = 0.08$ GeV for the parallel direction.
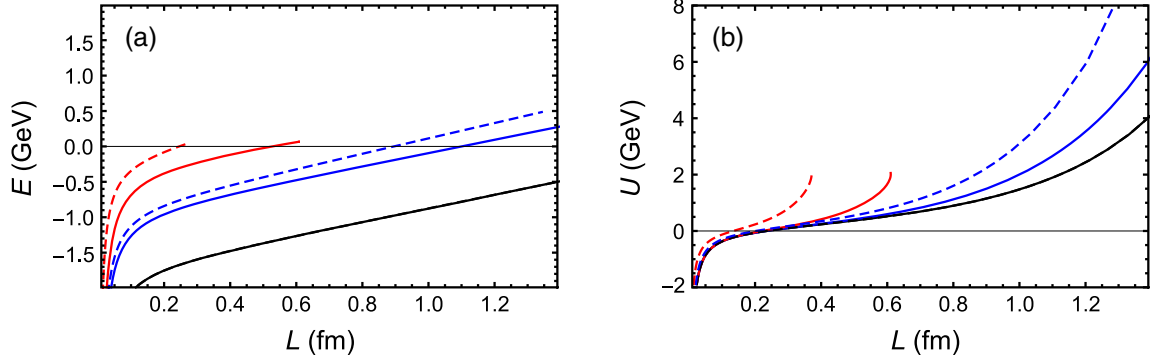
FIG. 3.   (a) The dependence of binding energy on L for different ω. The chemical potential is 0, and the temperature is $T = 0.1$ GeV. The black line is $\omega = 0$, the blue line is $\omega = 0.05$ GeV, and the red line is $\omega = 0.08$ GeV for the transverse direction. The black dashed line is $\omega = 0$, the blue dashed line is $\omega = 0.05$ GeV, and the red dashed line is $\omega = 0.08$ GeV for the parallel direction. (b) The dependence of internal energy on L for different ω. The chemical potential is 0, and the temperature is $T = 0.1$ GeV. The black line is $\omega = 0$, the blue line is $\omega = 0.05$ GeV, and the red line is $\omega = 0.08$ GeV for the transverse direction. The black dashed line is $\omega = 0$, the blue dashed line is $\omega = 0.05$ GeV, and the red dashed line is $\omega = 0.08$ GeV for the parallel direction.

dissolution [11]. It can be found that the quarkonium will dissociate more easily by increasing the angular velocity ω. The entropic force can be easily calculated from the $F_e = T\partial S/\partial L$ as in Fig. 2(b), and the entropic force will go to infinite when approaching the screening distance. For the same distance, the quark-antiquark pair in the parallel direction will feel larger entropic force than that in the transverse direction.

From the definition of binding energy, we compute the dependence of binding energy of heavy $Q\bar{Q}$ pair on the interquark distance L of the $Q\bar{Q}$ pair at different angular velocities ω in Fig. 3(a). With the increase of ω, the binding energy increases quickly to zero as compared to the $\omega = 0$ limit at fixed temperature. Note that $E_{Q\bar{Q}}(L_c) = 0$ at some value $L_c < L_{\text{screening}}$, but this does not imply that the $Q\bar{Q}$ pair dissociates at this length scale as discussed in Ref. [63]. The $Q\bar{Q}$ pair might be metastable even beyond L_c.

The dependence of internal energy of heavy $Q\bar{Q}$ pair on the interquark distance L of the $Q\bar{Q}$ pair at different angular velocities ω is drawn in Fig. 3(b). For small distance L, the behavior of the internal energy is nearly the same at different ω. However, for large distance L, the internal energy becomes large with the increase of ω. This difference is mainly due to the contribution of entropy for different ω. From above study, we find the angular velocity will have little influence on maximum internal energy in different directions.

IV. FREE ENERGY, ENTROPY, AND INTERNAL ENERGY OF SINGLE QUARK

The free energy, entropy, and internal energy of single quark can be calculated from the formula of heavy quarkonium by choosing the integrate range form 0 to z_h. The conformal case of single quark can be easily calculated as [63]

$$F_Q = -\frac{\sqrt{\lambda}}{2}T, \qquad S_Q = \frac{\sqrt{\lambda}}{2}, \qquad U_Q = 0. \quad (28)$$

λ is set to be 1 as before. The free energy, entropy, and internal energy of a single quark in this model is shown in Fig. 4 for different angular velocities. Since it is a single quark, there is no difference for different directions. The value of F_Q/T will tend to the conformal case $-1/2$ with the increase of temperature for different angular velocities. The increase of angular velocity will let F_Q/T decrease quickly with the temperature. Similarly, the entropy will tend to the conformal case $1/2$, and the internal energy
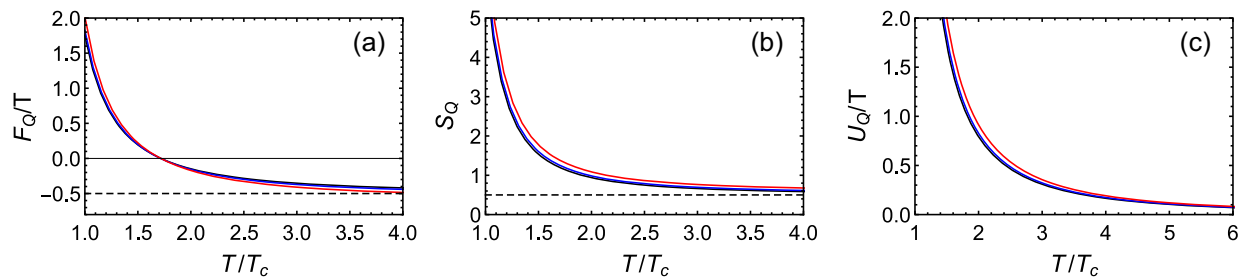

FIG. 4.   (a) Free energy of single quark as a function of T. (b) Entropy of single quark as a function of T. (c) Internal energy of single quark as a function of T. The black line is $\omega = 0$, the blue line is $\omega = 0.03$, and the red line is $\omega = 0.05$ for vanishing chemical potential.

will tend to zero at large T for different angular velocities. For the fixed temperature, the entropy and internal energy will increase with the increase of angular velocity. These three figures exhibiting thermodynamic quantities have a strong dependence on the temperature. The free energy, entropy, and internal energy of single quark are a decreasing function of temperature. Besides, it appears that the angular velocity plays a very small role in Fig. 4. This phenomenon relates to the competition of temperature and rotation. The temperature for the systems of single quarks is extremely high; thus, the effect of rotation will be suppressed and vice versa.

V. CONCLUSIONS

In this paper, we extend the deformed AdS Schwarzschild black hole to the rotating background with planar horizon by using the method proposed in Refs. [53,54,56,57]. Then, we use the rotating background to heavy quarkonium. It is found that the interquark distance L cannot go to infinity at large angular velocity, which means finite angular velocity will change the system from the confinement phase to the deconfinement phase. In the deconfinement phase, the heavy quarkonium will have a certain screening length. This is clearly shown in the figure of free energy. The entropy has been calculated in this paper. The entropic force induced by entropy may play an important role in the dissolution of heavy quarkonium. We find that large angular velocity will lead to a quick increase of entropy versus L. Mainly due to the entropic contribution, the internal energy will have a difference at large angular velocity for large L. Large angular velocity will drive the absolute value of binding energy to decrease quickly with the increase of L. But we should note the L_c is not the screening distance, when $E_{Q\bar{Q}}(L_c) = 0$. The quark-antiquark pair will become a metastable state beyond L_c.

For a comparison, we also show the string is parallel and transverse to the rotation direction. We can see that different directions do not affect the maximum value of free energy, entropy, binding energy, and internal energy. But the maximum value will happen at small distance for the parallel direction.

At last, we calculate the free energy, entropy, and internal energy of a single quark. These qualities are a decreasing function of the temperature. For the different angular velocities, all values of F_Q/T in the large T will tend to the conformal case $-1/2$. Large angular velocity will drive the free energy decrease quickly with the increase of temperature. The entropy and internal energy will be enhanced with the increase of angular velocity. At large T, the entropy and internal energy will tend to $\frac{1}{2}$ and 0, respectively.

[1] K. Adcox *et al.* (PHENIX Collaboration), Nucl. Phys. A757, 184 (2005).
[2] J. Adams *et al.* (STAR Collaboration), Nucl. Phys. A757, 102 (2005).
[3] I. Arsene *et al.* (BRAHMS Collaboration), Nucl. Phys. A757, 1 (2005).
[4] M. L. Miller, K. Reygers, S. J. Sanders, and P. Steinberg, Annu. Rev. Nucl. Part. Sci. 57, 205 (2007).
[5] T. Matsui and H. Satz, Phys. Lett. B 178, 416 (1986).
[6] N. Brambilla, A. Pineda, J. Soto, and A. Vairo, Rev. Mod. Phys. 77, 1423 (2005).
[7] N. Brambilla, J. Ghiglieri, A. Vairo, and P. Petreczky, Phys. Rev. D 78, 014017 (2008).
[8] O. Kaczmarek, F. Karsch, P. Petreczky, and F. Zantow, Phys. Lett. B 543, 41 (2002).
[9] P. Petreczky and K. Petrov, Phys. Rev. D 70, 054503 (2004).
[10] O. Kaczmarek and F. Zantow, *Proc. Sci.*, LAT2005 (2006) 192 [arXiv:hep-lat/0510094].
[11] D. E. Kharzeev, Phys. Rev. D 90, 074007 (2014).
[12] K. Hashimoto and D. E. Kharzeev, Phys. Rev. D 90, 125012 (2014).
[13] I. Iatrakis and D. E. Kharzeev, Phys. Rev. D 93, 086009 (2016).

[14] K. B. Fadafan and S. K. Tabatabaei, Phys. Rev. D 94, 026007 (2016).
[15] Z. Zhang, C. Ma, D. Hou, and G. Chen, arXiv:1611.08011.
[16] Z. Zhang, D. Hou, Z. Luo, and G. Chen, Adv. High Energy Phys. 2017, 8910210 (2017).
[17] Z. Zhang and D. Hou, Phys. Lett. B 803, 135301 (2020).
[18] Z. q. Zhang, Phys. Rev. D 101, 106005 (2020).
[19] Z. q. Zhang, D. f. Hou, and G. Chen, Phys. Lett. B 768, 180 (2017).
[20] H. Satz, Eur. Phys. J. C 75, 193 (2015).
[21] Z. T. Liang and X. N. Wang, Phys. Rev. Lett. 94, 102301 (2005); 96, 039901(E) (2006).
[22] X. G. Huang, P. Huovinen, and X. N. Wang, Phys. Rev. C 84, 054910 (2011).
[23] F. Becattini, F. Piccinini, and J. Rizzo, Phys. Rev. C 77, 024906 (2008).
[24] L. P. Csernai, V. K. Magas, and D. J. Wang, Phys. Rev. C 87, 034906 (2013).
[25] Y. Jiang, Z. W. Lin, and J. Liao, Phys. Rev. C 94, 044910 (2016); 95, 049904(E) (2017).
[26] W. T. Deng and X. G. Huang, Phys. Rev. C 93, 064907 (2016).

[27] L. G. Pang, H. Petersen, Q. Wang, and X. N. Wang, Phys. Rev. Lett. **117,** 192301 (2016).

[28] J. M. Maldacena, Int. J. Theor. Phys. **38,** 1113 (1999).

[29] S. Gubser, I. R. Klebanov, and A. M. Polyakov, Phys. Lett. B **428,** 105 (1998).

[30] E. Witten, Adv. Theor. Math. Phys. **2,** 253 (1998).

[31] J. Casalderrey-Solana, H. Liu, D. Mateos, K. Rajagopal, and U. A. Wiedemann, arXiv:1101.0618.

[32] O. DeWolfe, S. S. Gubser, C. Rosen, and D. Teaney, Prog. Part. Nucl. Phys. **75,** 86 (2014).

[33] O. Andreev and V. I. Zakharov, Phys. Rev. D **74,** 025023 (2006).

[34] O. Andreev and V. I. Zakharov, Phys. Lett. B **645,** 437 (2007).

[35] O. Andreev and V. I. Zakharov, J. High Energy Phys. 04 (2007) 100.

[36] P. Colangelo, F. Giannuzzi, and S. Nicotri, Phys. Rev. D **83,** 035015 (2011).

[37] X. Chen, S. Feng, Y. Shi, and Y. Zhong, Phys. Rev. D **97,** 066015 (2018).

[38] O. DeWolfe, S. S. Gubser, and C. Rosen, Phys. Rev. D **83,** 086005 (2011).

[39] Y. Yang and P. Yuan, J. High Energy Phys. 11 (2014) 149.

[40] Y. Yang and P. Yuan, J. High Energy Phys. 12 (2015) 161.

[41] X. Chen, D. Li, and M. Huang, Chin. Phys. C **43,** 023105 (2019).

[42] X. Chen, D. Li, D. Hou, and M. Huang, J. High Energy Phys. 03 (2020) 073.

[43] R. G. Cai, S. He, and D. Li, J. High Energy Phys. 03 (2012) 033.

[44] B. McInnes, Nucl. Phys. **B887,** 246 (2014).

[45] M. M. Caldarelli, G. Cognola, and D. Klemm, Classical Quantum Gravity **17,** 399 (2000).

[46] J. Sonner, Phys. Rev. D **80,** 084031 (2009).

[47] A. N. Atmaja and K. Schalm, J. High Energy Phys. 04 (2011) 070.

[48] B. McInnes, Nucl. Phys. **B861,** 236 (2012).

[49] B. McInnes, Nucl. Phys. **B864,** 722 (2012).

[50] B. McInnes, Classical Quantum Gravity **31,** 025009 (2014).

[51] B. McInnes and E. Teo, Nucl. Phys. **B878,** 186 (2014).

[52] J. Lemos, Phys. Lett. B **353,** 46 (1995).

[53] A. M. Awad, Classical Quantum Gravity **20,** 2827 (2003).

[54] M. B. Gaete, L. Guajardo, and M. Hassaine, J. High Energy Phys. 04 (2017) 092.

[55] H. Nadi, B. Mirza, Z. Sherkatghanad, and Z. Mirzaiyan, Nucl. Phys. **B949,** 114822 (2019).

[56] C. Erices and C. Martinez, Phys. Rev. D **97,** 024034 (2018).

[57] X. Chen, L. Zhang, D. Li, D. Hou, and M. Huang, arXiv: 2010.14478.

[58] M. Natsuume, Lect. Notes Phys. **903,** 1 (2015).

[59] Q. H. Zhang, arXiv:hep-ph/0106242.

[60] K. B. Fadafan, H. Liu, K. Rajagopal, and U. A. Wiedemann, Eur. Phys. J. C **61,** 553 (2009).

[61] M. Ali-Akbari and K. B. Fadafan, Nucl. Phys. **B835,** 221 (2010).

[62] J. Sadeghi and B. Pourhassan, Int. J. Theor. Phys. **50,** 2305 (2011).

[63] C. Ewerz, O. Kaczmarek, and A. Samberg, J. High Energy Phys. 03 (2018) 088.

[64] O. Kaczmarek and F. Zantow, Phys. Rev. D **71,** 114510 (2005).

[65] O. Kaczmarek and F. Zantow, arXiv:hep-lat/0506019.

[66] J. Zhou, X. Chen, Y. Q. Zhao, and J. Ping, Phys. Rev. D **102,** 086020 (2020).